

Multinuclear Quadrupole Resonance Studies of Biological Systems

Yukio Hiyama

Upjohn Tsukuba Laboratories, 23 Wadai, Tsukuba, Ibaraki 300-42 Japan

Z. Naturforsch. **45a**, 273–292 (1990); received August 22, 1989

We have employed multinuclear quadrupole resonance, using the field cycling technique, to study the structure of heterocyclic biomolecules. The electron density at nitrogen was investigated by the Townes-Dailey model of ^{14}N NQR. Large substituent effects were evident especially on the π orbitals. Electron transfer through H-bonds also affects the ^{14}N quadrupole interaction. Deuterium quadrupole resonance at exchangeable sites was also utilized. Since the deuterium quadrupole correlation coefficient is sensitive to the geometry of H-bonds, the intermolecular distance of the pyrrole-pyridine complex could be determined. The field cycling technique is sensitive enough to detect $^{14}\text{N} \cdots ^{14}\text{N}$ double transitions in parabanic acid thanks to the long spin-lattice relaxation time. However in many biological systems, such as hydrates, the technique is hardly applicable because of the short proton relaxation times. In such cases the solid state NMR technique was utilized. The ^2H NMR spectrum of thymidine reveals interesting static and dynamical features of deuterium quadrupole interaction.

Introduction

NQR spectroscopy [1], especially of ^{14}N , has a great potential for the study of biomolecules. The double resonance technique [2, 3] has made it possible to observe NQR signals from light nuclei such as ^2H , ^{10}B , ^{11}B , ^{14}N , ^{17}O , ^{23}Na , ^{25}Mg . Those nuclei are hardly detectable by single-resonance methods because of the low transition frequencies resulting in weak signals [4–9].

Since Edmonds and Speight reported ^{14}N NQR spectra of amino acids [10] and nucleoside bases [11], some more studies [3, 11–13] on biochemical systems have provided valuable information. In the first half of this paper, ^{14}N NQR spectra of a family of 21 heterocyclic compounds are presented to add to the existing data base [1, 3, 6, 14–19]. The series embodies wide variations in ^{14}N environment in terms of the atoms that make up the ring, and also provides variation in H-bonding environments. The effect of various substituents on amino and imino nitrogen yields the change of the π electron densities through Townes-Dailey analysis. The H-bond effect on the ^{14}N electric field gradient (EFG) tensor is also presented. H-bond geometries can be estimated from the correlation of the deuterium quadrupole coupling constants

(DQCC's) with $\text{N} \cdots \text{O}$, $\text{O} \cdots \text{O}$ or $\text{N} \cdots \text{N}$ distances [20–22]. In the second part of the paper, the dynamics of biomolecules will be discussed. The field cycling NQR spectroscopy relies on the relaxation behavior of the proton spin system. When the relaxation time is long, weak quadrupole resonance signals, such as that from ^{17}O in natural abundance, can be detected since the signals are actually detected as remaining proton magnetization [3]. On the other hand, the field cycling itself destroys usable proton magnetization, making the field cycling experiments difficult when the relaxation time is short. Two extreme examples are presented. In the last part of the paper, motional averaging in H-bonded systems will be discussed.

Theory

In zero field, NQR transitions are observed between nuclear energy levels determined by the quadrupole Hamiltonian

$$H_Q = \frac{e^2 Q q_{zz}}{4S(2S-1)} [3S_z^2 - S^2 + (\eta/2)(S_+^2 + S_-^2)]. \quad (1)$$

$e^2 Q q_{zz}/h$ is the quadrupole coupling constant, S the nuclear spin and η the asymmetry parameter. The EFG, q , is a traceless second order tensor. In the principal axis system the EFG is diagonal; by convention the axis system is defined so that $|q_{zz}| \geq |q_{yy}| \geq |q_{xx}|$. The asymmetry parameter, defined as $\eta = (q_{xx} - q_{yy})/q_{zz}$, ranges from 0 to 1. The asymmetry parameter and

Presented at the Xth International Symposium on Nuclear Quadrupole Resonance Spectroscopy, Takayama, Japan, August 22–26, 1989.

Reprint requests to Dr. Y. Hiyama, Upjohn Tsukuba Laboratories, 23 Wadai, Tsukuba, Ibaraki 300-42, Japan.

0932-0784 / 90 / 0300-0273 \$ 01.30/0. – Please order a reprint rather than making your own copy.



Dieses Werk wurde im Jahr 2013 vom Verlag Zeitschrift für Naturforschung in Zusammenarbeit mit der Max-Planck-Gesellschaft zur Förderung der Wissenschaften e.V. digitalisiert und unter folgender Lizenz veröffentlicht: Creative Commons Namensnennung-Keine Bearbeitung 3.0 Deutschland Lizenz.

Zum 01.01.2015 ist eine Anpassung der Lizenzbedingungen (Entfall der Creative Commons Lizenzbedingung „Keine Bearbeitung“) beabsichtigt, um eine Nachnutzung auch im Rahmen zukünftiger wissenschaftlicher Nutzungsformen zu ermöglichen.

This work has been digitalized and published in 2013 by Verlag Zeitschrift für Naturforschung in cooperation with the Max Planck Society for the Advancement of Science under a Creative Commons Attribution-NoDerivs 3.0 Germany License.

On 01.01.2015 it is planned to change the License Conditions (the removal of the Creative Commons License condition “no derivative works”). This is to allow reuse in the area of future scientific usage.

the quadrupole coupling constant completely describe the EFG tensor in the principal axis system. For $S=1$, the eigenfunctions and energy levels for the Hamiltonian in terms of the eigenfunctions of S_z are

$$\begin{aligned} |Y\rangle &= (1/\sqrt{2})\{|+1\rangle + |-1\rangle\}: & e^2 Q q_{zz}(1+\eta)/4h, \\ |X\rangle &= (1/\sqrt{2})\{|+1\rangle - |-1\rangle\}: & e^2 Q q_{zz}(1-\eta)/4h, \\ |Z\rangle &= |0\rangle: & -e^2 Q q_{zz}/2h, \end{aligned} \quad (2)$$

There are three transitions at

$$\begin{aligned} \nu_+ &= 3e^2 Q q_{zz}(1+\eta/3)/4h, \\ \nu_- &= 3e^2 Q q_{zz}(1-\eta/3)/4h, \\ \nu_0 &= e^2 Q q_{zz}\eta/2h, \end{aligned} \quad (3)$$

corresponding to $|Y\rangle \leftrightarrow |Z\rangle$, $|X\rangle \leftrightarrow |Z\rangle$, $|Y\rangle \leftrightarrow |X\rangle$, respectively.

The Townes-Dailey model [1, 23] provides a means of relating the population of the nitrogen valence orbitals to the ^{14}N NQR data [24, 25]. The valence orbitals in the case of the pyrrole nitrogen are those involved in the N-H σ , N-C σ , and π bonds. The appropriate relations between EFG parameters and populations of these orbitals are

$$\begin{aligned} \frac{e^2 Q q_{zz}/h}{e^2 Q q_{210}/h} \cdot \eta &= 3(1 - \cot^2 \gamma)(\sigma_{\text{NH}} - \sigma_{\text{NC}})/2 \propto \nu_0, \\ \frac{e^2 Q q_{zz}/h}{e^2 Q q_{210}/h} (1 + \eta/3) &= \pi - \sigma_{\text{NC}} \propto \nu_+, \end{aligned} \quad (4)$$

where $e^2 Q q_{210}$ is the ^{14}N NQCC due to a single valence 2p electron (we choose the value -9.1 MHz), 2γ is the C-N-C bond angle, and σ_{NH} , σ_{NC} , and π are the populations of the indicated nitrogen orbitals. These expressions are based upon the assumption that the ^{14}N EFG tensor orientation in pyrrole is identical to that determined for N-acetylvaline by a single-crystal ^{14}N NMR study [26]. The character of the fine structure in the CP/MASS ^{13}C - ^{14}N dipolar coupling [28], confirms this orientation assignment, which leads to a negative sign of the quadrupole coupling constant. From these observations it is possible to conclude that the relative order of the nitrogen valence orbital populations is $\pi > \sigma_{\text{NH}} > \sigma_{\text{NC}}$.

For the pyridine type of nitrogen the EFG parameters are related to the population of the lone-pair orbital, σ_{LP} , as well as to the population of the nitrogen orbitals involved in the σ and π bonds to carbon:

If $\sigma_{\text{LP}} > \sigma_{\text{NC}} > \pi$:

$$\begin{aligned} \frac{e^2 Q q_{zz}/h}{e^2 Q q_{210}/h} \eta &= 3(\sigma_{\text{NC}} - \pi)/2 \propto \nu_0, \\ \frac{e^2 Q q_{zz}/h}{e^2 Q q_{210}/h} (1 - \eta/3) &= (1 - \cot^2 \gamma)(\sigma_{\text{LP}} - \sigma_{\text{NC}}) \propto \nu_-; \end{aligned} \quad (5-1)$$

the Y axis is normal to the molecular plane.

If $\sigma_{\text{LP}} > \pi > \sigma_{\text{NC}}$:

$$\begin{aligned} \frac{e^2 Q q_{zz}/h}{e^2 Q q_{210}/h} \eta &= 3(\pi - \sigma_{\text{NC}})/2 \propto \nu_0, \\ \frac{e^2 Q q_{zz}/h}{e^2 Q q_{210}/h} (1 + \eta/3) &= (1 - \cot^2 \gamma)(\sigma_{\text{LP}} - \sigma_{\text{NC}}) \propto \nu_+; \end{aligned} \quad (5-2)$$

the X axis is normal to the molecular plane.

The latter case will be found in a π -electron rich imino nitrogen in nucleoside bases.

Experimental

All compounds were obtained from commercial sources and were used without further purification. Deuteration of parabanic acid, hydantoin, thiohydantoin and allantoin was carried out by recrystallization from D_2O . The experimental procedures in the double resonance level crossing (DRLC) method, and the spectrometers used in this work are described elsewhere [29–31]. The amount of sample in each case was of the order 0.2 to 5 g.

Solid state ^2H NMR spectra were recorded either at 38.45 MHz or at 76.76 MHz. The spectrometers were described elsewhere [32, 33].

Results and Discussion

1. ^2H and ^{14}N NQR of Heterocyclics

^{14}N NQR Results

Preliminary measurements of ^1H T_1 were carried out for all compounds at 77 K; a few additional measurements were made at room temperature. The T_1 values ranged from 20 s to several minutes, long enough to satisfy the adiabatic condition necessary for the DRLC experiments. The long ^1H relaxation times indicated absence of molecular motion in these crystals. Strong ^1H NMR signals were observed after the remagnetization. All ^{14}N NQR data obtained in this work are listed in Table 1.

Table 1. Nitrogen-14 nuclear quadrupole resonance spectra.

Compound site	Temp. (K)	ν_+	ν_-	ν_0	$e^2 Q q_{zz}/h$	η
1. Parabanic acid						
NH(1)	77	2422.0(1)	1932.5(3)	488.8(2)	2903.7(2)	0.3367(3)
NH(2)		2446.4(1)	1947.5(3)	499.0(2)	2929.3(3)	0.3407(3)
2. Uric acid						
N(1)H	77	2555 (2)	1760 (4)	795 (2)	2877 (6)	0.553 (4)
N(3)H		2895 (2)	1990 (4)	905 (2)	3257 (6)	0.556 (4)
N(7)H		2695 (2)	1895 (4)	800 (2)	3060 (6)	0.523 (4)
N(9)H		2610 (2)	1705 (4)	905 (2)	2877 (6)	0.629 (4)
3. Hydantoin						
(O)-NH-(O)	77	2264 (2)	1860 (4)	410 (2)	2745 (6)	0.299 (4)
(O)-NH-(CH ₂)		3190 (2)	2480 (4)	740 (2)	3760 (6)	0.394 (4)
Hydantoin deuterated weak signals/2290(10), 3200(10)						
4. Thiohydantoin						
(S)-NH-(O)	77	2248 (2)	1730 (4)	520 (2)	2652 (6)	0.392 (4)
	300	2270 (5)		540 (5)	2667(10)	0.405(10)
(S)-NH-(CH ₂)	77	2867 (2)	2170 (4)	698 (2)	3358 (6)	0.416 (4)
	300	2880 (5)		740 (5)	3347(10)	0.442(10)
5. Allantoin						
NH ₂	77	3720 (2)	2870 (4)	790 (2)	4393 (6)	0.360 (4)
NH(1)		2330 (2)	1870 (4)	460 (2)	2800 (6)	0.329
NH(2)		3210 (2)	2660 (4)	560 (2)	3913 (6)	0.286
NH(3)		2930 (2)	2280 (4)	630 (2)	3473 (6)	0.363 (4)
6. Allantoic acid hemihydrate						
NH ₂ (1)	77	2900 (2)	2254 (4)	630 (2)	3433 (6)	0.379 (4)
NH ₂ (2)		3050 (2)	2550 (4)	480 (2)	3733 (6)	0.268 (4)
-NH-(1)		3550 (2)	2770 (4)	780 (2)	4213 (4)	0.370 (4)
-NH-(2)		3630 (2)	2850(10)	780 (2)	4320 (6)	0.361 (4)
7. 1H-Benzotriazole						
-NH-		2588 (2)	1530(10)	1060 (5)	2745	0.772
		2415 (2)	1233(10)	1185 (5)	2432	0.974
		2342 (2)	1420(20)	925(10)	2508	0.738
		2315 (2)	1400(20)	925(10)	2478	0.747
-N(3)=		3350 (5)	ν_0 lines; 760(10), 660(10), 460(10)		3760-4160	0.22-0.40
		3200 (5)				
8. 1H-Indazole						
-NH-	77	3100 (2)	1740 (4)	1370 (2)	3227 (6)	0.824 (4)
-N=		3860 (2)	2700 (4)	1160 (2)	4440 (6)	0.523 (4)
9. Hydroxybenzimidazole						
-NH-	300	2630 (5)	-	670 (5)	3066(10)	0.430 (8)
	77	2640 (1)	1975 (1)	665 (1)	3077 (1)	0.432
10. Mercaptobenzoxazole						
-NH-	77	2330 (2)	1780 (4)	550 (2)	2740 (6)	0.402 (4)
11. Benzoxazolinone						
-NH-	77	2730 (1)	2050 (1)	680 (1)	3187 (1)	0.427
	205	2735 (2)	2080 (4)	675 (2)	3197 (6)	0.422 (4)
12. Benzothiazol						
-N=	77	3070 (2)	-	310 (4)	3887(10)	0.16 (1)
13. Oxindole						
-NH-	77	2400 (2)	1750 (4)	650 (2)	2767 (6)	0.470 (4)
14. Benzoxazol						
-N=	77	2835 (3)	2764 (1)	80(20)	3733 (4)	0.038 (4)
15. α-Pyridoin						
-N=	77	3160 (2)	2765 (4)	395 (2)	3950 (6)	0.200 (4)
16. Pyrazole^b						
-N=	77	3665 (1)	2120 (5)	1545(10)	3857 (4)	0.801 (5)
		3640 (1)	2070 (5)	1565 (5)	3807 (4)	0.825 (5)
-NH-		2315 (1)	1465 (5)	850 (1)	2520 (1)	0.675
		2365 (1)	1415 (5)	950 (1)	2520 (1)	0.754
deutrated ^d						
		2323.5				
		2373.5				
17. Maleimide						
-NH-	77	2380 (1)	2138 (1)	242 (1)	3012 (1)	0.161
18. 7 Azaindole^e						
-NH-	77	2080(10)				
		2200(10)				
-N=		2850(10)				
		2935(10)				
20. Quinoline						
-N=	77	3740(20)	-	750(20)	4486(20)	0.33 (1)
21. Isoquinoline						
-N=	77			900(10)		
22. Cyanuric acid^c						
-NH-	77	2792 (1)	2038 (1)	754 (1)	3220 (2) ^f	0.468 (1)
		2783 (1)	1984 (1)	799 (1)	3178 (2)	0.503 (1)

^a in kHz^b Schempp and Bray reported ¹⁴N NQR frequencies at 3664.86, 3639.68, 2365.30, 2314.85, 2118.18 and 2073.67 kHz [17a]. Tarimoi and Schempp reported at 3664.9, 3639.7, 2365.3, 2314.0, 2118.2, 2073.8, 1566.5, 1546.7, 1423.0, 1465.1, 900.2 and 891.8 kHz [17b].^c Subbarao and Bray [J. Chem. Phys. **67**, 1085 (1977)] reported ν_+ and ν_- frequencies at 2791, 2783, 2039 and 1980 kHz.^d Deutrium satellites observed at 2436.0, 2494.6, 2453.5 and 2508.0 kHz.^e Insufficient data.^f weaker signals.

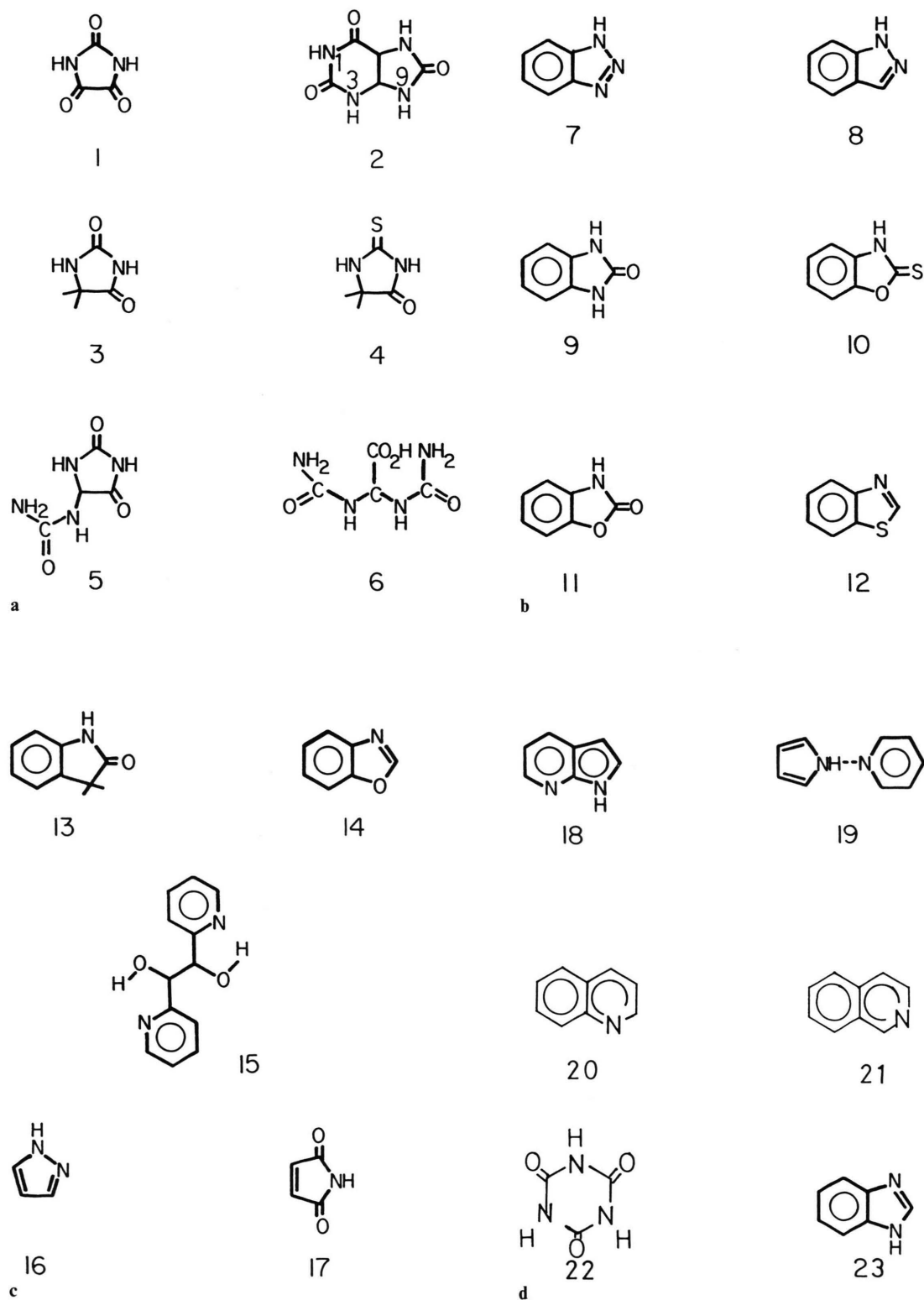


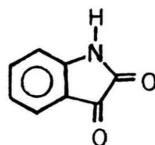
Fig. 1. Molecular schemes of heterocyclic compounds.



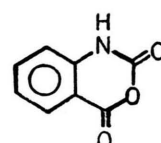
24



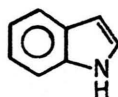
25



30



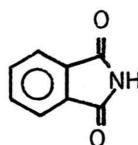
31



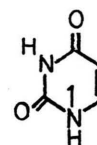
26



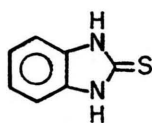
27



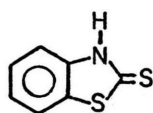
32



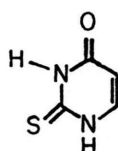
33



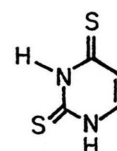
28



29



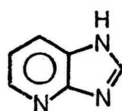
34



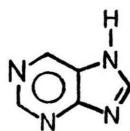
35

e

f



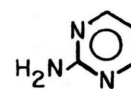
36



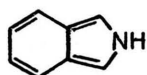
37



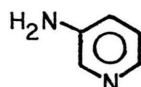
42



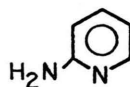
43



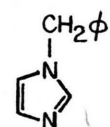
38



39



44



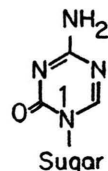
45



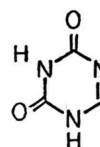
40



41



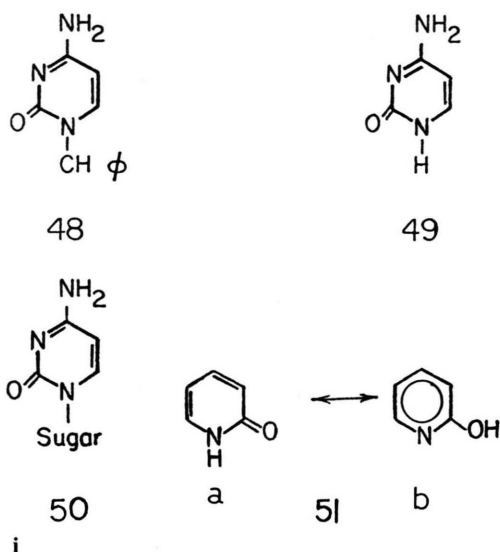
46



47

g

h



Parabanic Acid (1). A detailed scan, using 1 kHz increments with a static field (1.5×10^{-3} T) reduces the effects of ^1H satellites, permitted identification of 6 lines at 2447, 2422, 1948, 1934, 500, and 490 kHz. Thus there are two distinct nitrogens with similar EFG parameters, consistent with the X-ray and neutron diffraction results [34, 35].

Uric Acid (2). This compound gave four equally intense lines in the interval from 2500 to 2900 kHz, where the ν_+ transitions of aromatic amines commonly appear. The corresponding four ν_- lines and four ν_0 lines, (actually two broad lines overlapped), appear at 1700 through 2000 kHz, and 750 through 950 kHz, respectively. Therefore, the four different nitrogens [36] are distinguishable by ^{14}N NQR. Tentative assignments to individual sites are given later in this paper.

Hydantoin (3) and thiohydantoin (4). These two compounds are presumed to have an amine nitrogen with approximate sp^2 hybridization, and a second amine with approximate sp^3 . Nitrogen sites with distinctly different quadrupole coupling constants are thus expected, and are observed. The larger coupling constant is ascribed to the sp^3 type of amine site.

Allantoin (5). The electronic environments of the nitrogens in this compound should be closely similar to those in hydantoin. The NH_2 nitrogen transitions are readily assigned by noting the characteristic proton satellite structure. The $\text{NH}(1)$ is the sp^2 nitrogen in the ring. However, the sp^3 - NH - in the ring and the aliphatic $-\text{NH}-$'s are not distinguishable at this time.

Allantoic Acid (6). The NH_2 nitrogen transitions were readily distinguished due to the characteristic satellite features.

Benzotriazole (7). In the solid state structure of this compound there are four dependent molecules in the unit cell [37], so there should be twelve different nitrogen sites. All of the lines due to the amino nitrogen sites were observed and assigned, but only a few of the much less intense imino nitrogen transitions were detected.

Hydroxybenzimidazole (9). The ^{14}N NQR spectrum shows only one distinguishable set of ^{14}N transitions, suggesting that the molecule has C_2 symmetry like the molecule of mercaptobenzimidazole [38], for which the ^{14}N NQR spectrum was obtained earlier [19].

Mercaptobenzoxazole (10) and Benzoxazolinone (11). Only one set of quite intense signals, which are expected to be the amino nitrogen signals, was observed for each compound. These results are in good agreement with the structural data [39].

Benzothiazole (12), Oxindole (13), Benzoxazole (14). For these compounds there are no crystallographical data available. Rather weak and relatively high frequency ν_+ transitions, apparently due to imino nitrogens, were observed for benzothiazol and benzoxazol. On the other hand, the much more intense signals in the oxindole spectrum are more plausibly assigned to the amino nitrogen.

An interesting feature of the ^{14}N spectrum of benzoxazol is that the ν_- line is more intense than the ν_+ line, as shown in Figure 2. ν_+ lines are generally much more intense than ν_- in the ^{14}N DRLC spectrum [3]. Although one cannot ordinarily observe lines in the very low frequency range (≈ 100 kHz) due to intense proton absorption, it was possible to observe the ν_0 line by employing fairly long (12 s) irradiation times at zero field (Fig. 3).

α -Pyridoin (15). The molecular structure of this substance shows that there are intramolecular H-bonds involving alcohol hydrogen and imino nitrogen [40]. Although the ^{14}N signals might be expected to be more intense because of the resulting shorter hydrogen-nitrogen distance, the transitions were nevertheless quite weak, as is the case for the other imino nitrogens studied.

Pyrazole (16). The crystal and molecular structures show that there are two independent molecules in the unit cell of pyrazole [41, 42]. All twelve ^{14}N transitions were observed. There are, however, so many lines in

the 1400 to 1600 kHz interval that the uncertainties in the frequencies of the ν_0 lines of the imino nitrogens are unusually large. The results for the imino nitrogens differ from those reported previously [17], as indicated in the footnote of Table 1.

Maleimide (17). Only three resonance lines were observed for this compound. This means that there is only one chemically independent molecule in the unit cell. An attempt to obtain the ^{17}O NQR spectrum, which was successful [43] for the similar compound

phthalimide, was not successful due to the short T_{1D} of the protons.

Quinoline (20). The sample was dried through molecular 3 Å sieves because the commercial sample showed unfavorable T_1 behavior. Relatively weak and broad ^{14}N NQR resonances have been observed for the dried compound.

Cyanuric Acid (22). The crystallographic studies have shown that the molecule in the solid state has C_2 symmetry resulting in two inequivalent nitrogens [44].

The two inequivalent sites have been observed by the ^{14}N NQR. One is about twice as intense than the other site where the nitrogen lies along the C_2 axis. The NQR parameters for the two different sites are quite similar because they are almost equivalent except for the H-bond geometry.

^2H NQR results

The deuterium NQR data obtained here are listed in Table 2. Spectrum assignments for the compounds with more than one deuterium site have been performed with the aid of specific line shapes by a small static magnetic

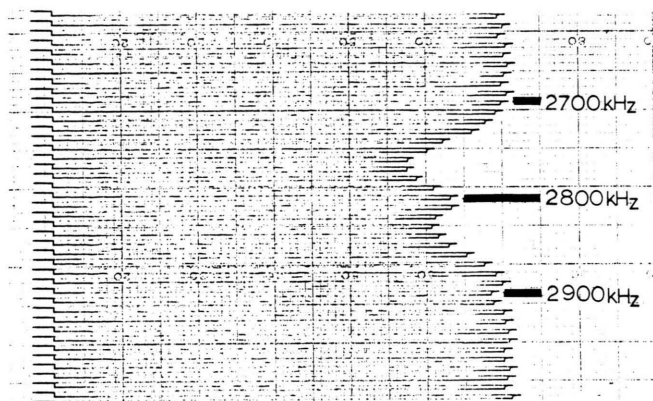


Fig. 2. Unusual relative intensities of ν_+ , ν_- lines of ^{14}N NQR in benzoxazole. Experimental cycle was 120 s. Irradiation (5 G) time was 3 s. No static field was applied.

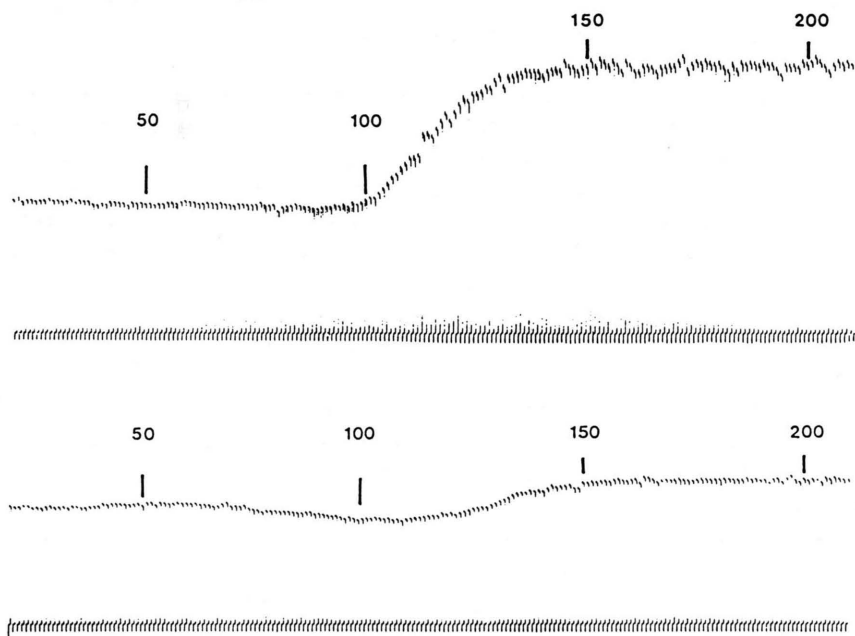


Fig. 3. ν_0 line of ^{14}N NQR in benzoxazole. The upper trace was taken with short irradiation (3 s) while the lower trace was obtained with long irradiation (15 s).

Table 2. Deuterium quadrupole resonance of N-D sites.

Substance	ν_+	ν_-	ν_0	$e^2 Q q_{zz}/h$	N ... O (Å)
1 Parabanic acid	151.0(2)	134.8(2)	190.5(2)	0.170	2.873 ^b
	144.8(2)	130.0(2)	183.2(2)	0.162	2.837
9 Hydroxybenzimidazole	141.0(5)	122.5(5)	175.7(5)	0.210	
10 Mercaptobenzoxazole	164.2(2)	151.2(2)	210.3(2)	0.124	weak ^c
11 Benzoxazolinone	149.6(1)	133.5(1)	188.7(1)	0.171	2.802 ^c
17 Maleimide*	148.5(2)	132.5(2)	187.3(2)	0.171	
22 Cyanuric acid	149.5(2)	134.0(2)	189.0(2)	0.164	2.7835 ^d
	139.0(2)	121.2(2)	173.4(2)	0.205	2.8051

* Two C-D sites observed at 152.0, 147.5, 134.5 and 132.5 kHz.

^a in kHz; ^b Ref. 34; ^c Ref. 39; ^d Ref. 45.Table 3. ¹⁴N NQR frequency in parabanic acid and in deuterated parabanic acid (* Ref. [34]).

Site	ν_+ (kHz)	
N(1)H	2422.0	N(1) ... O 2.837 Å*
N(2)H	2446.4	N(2) ... O 2.873 Å
N(1)D	2432	
N(2)H	2448	
N(1)H	2425	
N(2)D	2456	
N(1)D	2435	
N(2)D	2458	

field [45] and ¹⁴N-²H double flipping which would appear in the neighborhood of ¹⁴N transitions [21].

There are two different C-H deuterium sites observed in maleimide (17) in addition to the N-H deuterium site. This shows that the molecule has no C2 symmetry in the solid state while C2 symmetry would be expected in a free phase.

Deuterated cyanuric acid has given two N-H deuterium sites. The site with the lower DQCC (173.4 kHz) showed twice the absorption intensity of the other, so that this should correspond to the two equivalent deuterium sites which have longer N—O H-bond distance. Although this is not consistent with the empirical relationship between DQCC's and N—O H-bond distances [21], the two equivalent sites take a more favorable N—O—C angle, close to 120°, than the other to form the stronger H-bond.

The ²H spectrum of parabanic acid was assigned by the ¹⁴N-²H double flipping transitions. The double flipping frequencies are 2562.0, 2564.0, 2577.5, 2579.5, 2590.5, 2592.5, 2607.0 and 2609.0 kHz. They are all doublets about 2 kHz apart. A careful scan in the ¹⁴N ν_+ frequency range has shown a complete set of

¹⁴N ν_+ frequencies, as listed in Table 3. It is noteworthy that the ν_+ frequencies of protonated NH sites in the halfly deuterated molecule are higher by about 2 kHz than those of the non-deuterated molecule. The change in ¹⁴N parameters upon deuteration was attributed to the crystal expansion by the deuteration [3].

Discussion

The characteristics of the ¹⁴N EFG tensor, including the orientation of the major principal axis, primarily depend upon the particular type of functional group represented by the nitrogen site, e.g., a pyrrole-like as opposed to a pyridine-like environment. Using the Townes-Dailey model, in conjunction with the orientation of the Z axis of the EFG tensor it is possible to extract from the NQR data, using (4) and (5), estimates of nitrogen valence orbital populations, or differences in the populations. We will employ the results of the Townes-Dailey analysis in the discussion that follows. Several necessary ¹⁴N NQR data for the discussion, which have been reported elsewhere, are listed in Table 4.

Effects of H-Bonding

It has been noted that the ¹⁴N QCC is considerably lower for the amino nitrogen of solid imidazole than for imidazole in the gas phase, or than for similar heterocyclic amino sites in other molecules in which H-bonding in the solid state is not present [17, 46–48]. There is considerable evidence in the spectroscopic and structural data for solid imidazole for relatively strong intermolecular N—H ... N H-bonding [49, 50].

The effect of H-bonding on the EFG parameters of the amino nitrogen can be understood by (4). The

Table 4. ^{14}N NQR spectra reported elsewhere.

Substance	Site	ν_+	ν_-	ν_0	$e^2 Q q_{zz}/h$	η	Ref.
23 Benzimidazole	—NH—	1860	1100	760	1973	0.770	b, c, s, u
	—N=	2590	2130	460	3147	0.292	
26 Indole	—NH—	2305	—	275	2890	0.190	d, *
27 Imidazole	—NH—	1417	719	698	1418	0.997	b, e, u*
	—N=	2556	2345.5	210.5	3253	0.135	
28 Mercaptobenzimidazole	—NH—	2340	1790	550	2750	0.40	g
29 Mercaptobenzothiazole	—NH—	2140	1520	620	2440	0.51	h
30 Isatin	—NH—	2540	2050	490	3060	0.32	h
31 Isatoic anhydride	—NH—	2790	—	750	3220	0.47	h
32 Phthalimide	—NH—	2280	1960	—	2872	0.226	i
33 Uracil	—NH—	2311	1573	733	2593	0.565	b, c, g, s
		2287	1620	667	2605	0.512	
34 2-Thiouracil	—NH—	2060	1250	810	2207	0.734	g, j
		2110	1430	680	2360	0.580	
35 Dithiouracil	—NH—	2030	—	850	2140	0.794	g
		1970	—	730	2140	0.682	
36 Azabenzimidazole	—N(7)H—	1917	1231	686	2077	0.991	c
	—N(9)=	2531	2130	401	3107	0.258	
	—N(3)=	3468	2910	558	4252	0.263	
37 Purine	—N(7)H—	1838	956	882	1863	0.947	c
	—N(1)=	3407	2958	449	4243	0.212	
	—N(3)=	3377	2850	527	4151	0.254	
	—N(9)=	2514	2017	497	3021	0.329	
39 3-Aminopyridine	—NH ₂	3138.2	2426.9	(711)	3710	0.3835	k
	—N=	3810.4	2934.4	(876)	4496	0.3896	
40 Pyrimidine	—N=	3755	2899	(856)	4436	0.386	l
41 Thiazole	—N=	3379	2902	(477)	4187	0.227	m
42 4-Aminopyridine	—NH ₂	2967.9	2291.7	(676)	3506	0.3857	k
	—N=	2915.5	2755.5	(161)	3781	0.085	
43 2-Aminopyrimidine	—NH ₂	2784	2358	(426)	3428	0.249	o, s
44 2-Aminopyridine	—NH ₂	2970.3	2355.2	(615)	3550	0.3465	k, n
	—NH=	2841.8	2776.1	(66)	3745	0.0351	
45 N-Benzylimidazole	—NCH ₂ ph	1776	1521	255	2198	0.784	p
	—N=	2780	2729	(51)	3679	0.022	
46 5-Azacytidine	—N sugar	2200	—	—	—	—	c
	—NH ₂	2140	1420	715	2373	0.603	
	—N(3)=	2740	—	620	3240	0.383	
	—N(5)=	2720	—	620	3243	0.386	
47 5-Azauracil	—N(1)H	2176	1605	563	2514	0.448	c
	—N(3)H	2409	1551	858	2640	0.650	
	—N(5)=	2671	1921	749	3061	0.489	
48 N-Benzylcytosine	—NCH ₂ ph	2320	2210	(110)	3020	0.073	c
	—NH ₂	2280	1595	685	2583	0.530	
	—N(3)=	2810	—	1085	3023	0.718	
49 Cytosine	—NH(1)	2028	1219	801	2165	0.740	b, c, q, s, t
	—NH ₂	2492	1922	570	2941	0.388	
	—N(3)=	2723	1570	1153	2862	0.806	
50 Cytidine	—N sugar	2356	—	—	—	—	c, s
	—NH ₂	2476	1974	502	2967	0.338	
	—N(3)=	2683	1463	1220	2769	0.883	
51 α -Pyridon	—NH—	1477	845	632	1548	0.816	r

* Data reconfirmed this time. ^a in kHz. ^b D. T. Edmonds and P. A. Speight, *J. Magn. Reson.* **6**, 265 (1972). ^c Ref. [11]. ^d Ref. [10]. ^e M. J. Hunt, A. L. Mackay, and D. T. Edmonds, *Chem. Phys. Lett.* **34**, 473 (1975). ^f Ref. [48]. ^g Ref. [19]. ^h Y. Hiyama, T. Maruizumi, and E. Niki, *Bull. Chem. Soc. Jpn.* **52**, 2752 (1979). ⁱ Ref. [43]. ^j Ref. c in Table 1. ^k R. Ikeda, S. Onda, D. Nakamura, and M. Kubo, *J. Phys. Chem.* **72**, 2501 (1968). ^l E. Schempp and P. J. Bray, *J. Chem. Phys.* **46**, 1186 (1967). ^m Ref. [14]. ⁿ M. Chao and E. Schempp, *Acta Cryst.* **B33**, 1557 (1977). ^o H. Negita, K. Shobata, and T. Kubo, *Bull. Chem. Soc. Japan*, **46**, 110 (1973). ^p C. I. H. Ashby, C. P. Cheng, and T. L. Brown, *J. Amer. Chem. Soc.* **100**, 6057 (1978). ^q Y. Hiyama, N. Watanabe, T. Maruizumi, and E. Niki, *Nippon Kagaku Kaishi*, **961** (1979). ^r Ref. [3] appendix. ^s Ref. [25]. ^t Ref. [16]. ^u Ref. [15].

population of the π orbital normal to the planar array of N–C and N–H bonds is higher than $\sigma_{\text{N–C}}$ and $\sigma_{\text{N–H}}$, the populations of the σ orbitals in the plane. Thus, the Z axis of the EFG tensor is orientated along the π orbital. Any increase in $\sigma_{\text{N–H}}$, occasioned by charge transfer from the electron pair donor in a H-bond, should result in a decrease in the QCC. At the same time, because σ_{NH} is larger than σ_{NC} , the deviation from axial symmetry along the Z axis should grow larger, so that η should increase.

Table 5 lists the results of a Townes-Dailey analysis for several amino sites in the heterocyclic systems, with listing of the heavy atom distances in those cases where H-bonding is present. From the NQR data (Tables 1 and 4) it is possible to calculate $(\sigma_{\text{NH}} - \sigma_{\text{NC}})$, assuming that $e^2 Q q_{210}/h$ is -9.1 MHz.

The quantity $(\sigma_{\text{NH}} - \sigma_{\text{NC}})$ is distinctly smaller for pyrrole and indole than for the other compounds listed in the Table. It is just these two compounds for which H-bonding is not a significant feature of the solid state structure. Thus, these results support the idea of an increase in σ_{NH} upon formation of the H-bond.

To obtain a clearer view of the changes in charge distribution at both the donor and acceptor nitrogen sites upon H-bond formation, it is desirable to observe the ^{14}N NQR data at both sites in the absence and presence of H-bonding. The pyrrole-pyridine complex (19) was well-suited for study in this regard, because each of the pure components is essentially free of H-bonding effect. In this system it is possible to observe not only the ^{14}N NQR spectra but also, upon deuteration, the ^2H spectrum of the deuterium in the H-bond.

Correlations of the DQCC with $\text{O} \cdots \text{O}$ distances in $\text{O–H} \cdots \text{O}$ H-bonds have been widely discussed in [20, 51]. Data are available also for $\text{N–H} \cdots \text{O}$ and for $\text{N–H} \cdots \text{N}$ systems [21, 22]. The general result is that the DQCC decreases markedly upon H-bond formation and is a smooth function of the heavy atom distance. Application of the DQCC datum for the pyrrole-pyridine complex (177 kHz) to this empirical relationship yields an estimated $\text{N} \cdots \text{N}$ distance in the complex of 2.92 Å. Ikuta et al. [52] have reported an ab initio calculation of the pyrrole-pyridine complex in which an optimized $\text{N} \cdots \text{N}$ distance of 2.90 Å was obtained.

Table 6 provides a listing of the ^{14}N NQR data and estimated orbital populations of relevance at the pyridine and pyrrole nitrogen sites in the free compo-

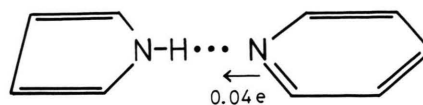


Fig. 4. Charge transfer through the H-bond in the pyrrole-pyridine complex.

Table 5. N–H populations and H-bond lengths.

Compound	$\sigma_{\text{NH}} - \sigma_{\text{NC}}$	Bond distances $\text{N} \cdots \text{O}$ $\text{N} \cdots \text{N}$
1 Parabanic acid	0.146	2.837 ¹
	0.142	2.873
4 Thiohydantoin	0.141	2.916 ²
5 Allantoin	0.125	2.827 ³
10 Mercaptobenzoxazole	0.160	weak NH—S bond
11 Benzoxazolinone	0.198	2.802 ⁴
26 Indole	0.070	no hydrogen bond
24 Pyrrole	0.080	no hydrogen bond
27 Imidazole	0.255	2.86 ⁵
23 Benzimidazole	0.253	2.90 ⁶

¹ Ref. [34]. ² L. A. Walker, K. Folting, and L. C. Merriitt, Jr., Acta Cryst. **B25**, 88 (1969). ³ D. Mootz, Acta Cryst. **19**, 726 (1965). ⁴ Ref. [39]. ⁵ Ref. [51] and Ref. [52]. ⁶ C. J. Dik-Edixhoven, H. Schenk, and H. van der Meer, Cryst. Struct. Comm. **2**, 23 (1973).

nents and in the complex. The shifts that occur in the NQR transition frequencies upon complex formation are quite evident. Concomitantly, there are shifts in the orbital populations. The resulting picture (Fig. 4) is one of a shift of about 0.04 e⁻ from the lone pair orbital of the pyridine to the N–H bond of the pyrrole nitrogen, along the $\text{N–H} \cdots \text{N}$ H-bond. A similar extent of charge transfer was noted in analysis of the ^{14}N data for a nucleotide pair involving and $\text{N–H} \cdots \text{N}$ H-bond [12].

Substituents Effect on Amino Nitrogen

As indicated in the theory section, the ν_+ frequency of ^{14}N NQR in amino nitrogens is proportional to the difference between π population and $\sigma_{\text{N–C}}$ population. The π population may be sensitive to substituents while the $\sigma_{\text{N–C}}$ population is rather constant. Therefore ν_+ frequencies can be good parameters to evaluate π population numbers for substituents effect. Also the ν_+ frequencies are relatively insensitive to H-bond geometry as listed in Table 7.

Taking ν_+ of pyrrole: 1685 kHz (see footnote of Table 6) as reference, changes in ν_+ of the amino nitrogens by various substituents are listed in Table 8. A 100 kHz increase in ν_+ corresponds to about 0.0148 e

Table 6. Nitrogen valence bond populations in pyrrole, pyridine, and the pyrrole-pyridine complex.

Substance	Site	e^2Qq/h^*	η	$\sigma_{\text{NH}} - \sigma_{\text{NC}}$	$\pi - \sigma_{\text{NC}}$	σ_{LP}
19 Pyrrole-Pyridine Complex ^a						
	—NH—	1833	0.588	0.15	0.24	—
	—N=	4287	0.364	—	—0.12	1.96
24 Pyrrole ^b	—NH—	2060	0.269	0.08	0.25	—
25 Pyridine ^c	—N=	4584	0.396	—	—0.13	2.00

* in kHz. ^a Ref. [44]. ^b Ref. [18]; the data were reconfirmed in the course of the present study. $\nu_+ = 1685.0$ kHz, $\nu_- = 1407.8$ kHz. ^c L. Guibe, Ann. Phys. 7, 177 (1962), averaged frequencies: $\nu_+ = 3892$ kHz, $\nu_- = 2984$ kHz, $\nu_0 = 909$ kHz.

Table 7. Hydrogen bond effect on ^{14}N ν_+ frequency of amino nitrogen.

Substance	ν_+	H-bond length	NQR Ref.
Parabanic acid	2446.4 2422.0	2.873 ^a 2.837	this work
Pyrrole	1684 1645	non hydrogen bond N...N 2.92 ^c	^b this work
Barbituric acid	2577 2568	2.90 ^d 2.80	^e
Cyanuric acid	2792 2783	2.7835 ^f 2.8051	this work
Alloxan	2670 2600	3.044 ^g 2.881	

^a Ref. [34]. ^b Ref. [18]. ^c this work. ^d W. Bolton, Acta Cryst. 16, 166 (1963). ^e E. A. Keiter, University of Illinois, unpublished. This result is not consistent with the data reported earlier (Ref. j in Table 4). ^f Ref. [45]. ^g C. Singh, Acta Cryst. 19, 759, (1965). ^h T. Maruizumi, Y. Hiyama, and E. Niki, Bull. Chem. Soc. Japan 53, 1443 (1980).

increase in the π orbital based upon the Townes and Dailey approximation.

Fused ring. The amino nitrogen in indole (26) has more electron than that in pyrrole (24). Also the π population of the amino nitrogen in benzimidazole (23) is substantially higher than that in imidazole (27). On the other hand, the π population of the nitrogen in phthalimide (32) is considerably lower than that in maleimide (17). Therefore one may conclude that the fused ring delivers π electrons to α position while the ring lessens π population density at β position. MO calculations have also shown that there is a substantial difference in the nitrogen π orbital populations between indole (26) and isoindole (38) [53–55]. The fused ring effects were also seen in azabenzimidazole (36) and in purine (37).

Imino group. The amino nitrogen in imidazole (27) has remarkably lower π population than that in pyrrole (24). The same trend is seen in benzimidazole (23) with respect to indole (26). As widely accepted, the imino nitrogen group withdraws π electrons considerably.

Exocyclic Oxygen. The amino nitrogen of maleimide (17) has two exocyclic oxygens at position α and ν_+ is higher by about 700 kHz than in pyrrole (24). Therefore, 350 kHz worth electron can be assigned to each exocyclic oxygen.

Cyclic Amino Nitrogen. One of the amino nitrogens of uracil has two α exocyclic oxygens and a β cyclic amino nitrogen. The difference between this and that in maleimide is just the β cyclic amino nitrogen. However, there is almost no difference in frequency between the two nitrogens. So this may suggest that there is not much effect on amino nitrogen by β amino nitrogen, which is quite reasonable considering that they are the same functional group.

The other amino nitrogen in uracil has α and γ exocyclic oxygens and β cyclic amino nitrogen and still has almost the same ν_+ as the first one. Therefore the γ exocyclic oxygen may be the same on cyclic amino nitrogen as the exocyclic oxygen.

Cyclic Oxygen and Sulfur. The difference between benzoxazolinone (11) and hydroxybenzimidazole (9) is the difference between the cyclic oxygen and the cyclic amino nitrogen. The ν_+ frequency of benzoxazolinone is higher by 90 kHz than that in hydroxybenzimidazole. So one may conclude that the β cyclic oxygen gave up 90 kHz worth π electron to the amino nitrogen. A similar comparison can be made between mercaptobenzimidazole (28) and mercaptobenzothiazole (29). The β -cyclic sulfur withdraws as much as 200 kHz worth π electron from the amino nitrogen.

Exocyclic Sulfur. ν_+ of mercaptobenzoxazole (10) is lower by 400 kHz than that in benzoxazolinone (11). So the exocyclic sulfur is almost neutral or a slightly π electron withdrawing group for the amino nitrogen.

The various substituent effects on the cyclic amino nitrogen are summarized in Table 9 and in Figure 5. Using the numbers in Table 9 one could calculate ν_+ for the various kinds of cyclic amino nitrogens as listed in Table 8. It is noteworthy that the calculated numbers are close to the experimentally observed numbers.

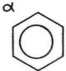
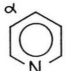
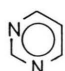
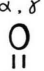
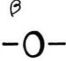

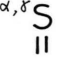
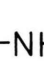

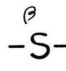
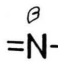
^{14}N NQR of α -pyridon (51) was reported earlier. ν_+ (1477 kHz) cannot be accounted for as a neutral amino nitrogen, which has been discussed above. In-

Table 8. Substituents effect on amino nitrogen by substances.

Substance	ph	-N=	-NH-	O 	S 	-O-	-S-	others	obs. Δv_+	calc. Δv_+	π el. (10^{-3})
24 Pyrrole ^c	-	-	-	-	-	-	-	-	0	0	0
26 Indole ^b	α	-	-	-	-	-	-	-	+621	+600	92
27 Imidazole ^b	-	β	-	-	-	-	-	-	-267	-270	-40
23 Benzimidazole ^b	α	β	-	-	-	-	-	-	+171	+330	+25
1 Parabanic Acid ^a	-	-	β	$2\alpha + \beta$	-	-	-	-	+750 ^d	+750	+111
9 Hydroxybenzimidazole	α	-	β	α	-	-	-	-	+956	+950	+142
10 Mercaptobenzoxazole	α	-	-	-	α	β	-	-	+646	+700	+96
11 Benzoxazolinone ^a	α	-	-	α	-	β	-	-	+1046	+1050	+155
17 Maleimide ^a	-	-	-	2α	-	-	-	-	+696	+700	+103
18 7-Azaindole ^a	-	-	-	-	-	-	-	*	+456	+450	+68
28 Mercaptobenzimidazole ^b	α	-	β	-	α	-	-	-	+656	+600	+97
29 Mercaptobenzothiazole ^b	α	-	-	-	α	-	β	-	+456	+450	+68
33 Uracil ^b	-	-	β	2α	-	-	-	-	+627	+700	+93
34 2-Thiouracil ^b	-	-	β	$\alpha + \gamma$	-	-	-	-	+603	+700	+89
35 Dithiouracil ^b	-	-	β	γ	α	-	-	-	+426	+350	+63
	-	-	β	α	α	-	-	-	+376	+350	+56
	-	-	β	-	$\alpha + \gamma$	-	-	-	+346	0	+51
32 Phthalimide ^b	β	-	-	2α	-	-	-	-	+286	0	+42
36 Azabenzimidazole ^b	-	β	-	-	-	-	-	*	+596	+600	+88
37 Purine ^b	-	β	-	-	-	-	-	**	+233	+180	+35
30 Isatin ^b	α	-	$\alpha + \beta$	-	-	-	-	-	+154	+130	+22
31 Isatoic Anhydride ^b	α	-	-	$\alpha + \gamma$	-	β	-	-	+856	+1000	+127
22 Cyanuric Acid	-	-	2β	$2\alpha + \beta$	-	-	-	-	+1106	+1400	+164
	-	-	-	-	-	-	-	-	+1104	+1050	+163

^a NQR data in Table 1. ^b NQR data in Table 4. ^c NQR data in Table 6, ^d averaged value. * α pyridine fused. ** α pyrimidine fused.

Table 9. π Electron donor capabilities on cyclic amino nitrogens. In e and in change of v_+ .

			α, δ 
0.089 600 kHz	0.067 450 kHz	0.059 400 kHz	0.052 350 kHz
β 	β 	α, δ 	-NH- 
0.015 100 kHz	0.007 50 kHz	0 0	0 0
β 	β 	β 	
-0.015 -100 kHz	-0.022 -150 kHz	-0.040 -270 kHz	

terestingly the ^{14}N NQR data are on the line of pyridinium cations, which have been extensively studied by Rubenacker et al. [56, 57].

Uric Acid assignment. The nitrogens in the six membered ring should be quite similar if the 5-membered

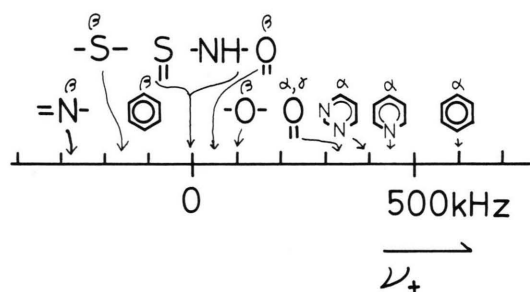


Fig. 5. π electron densities induced by substituents, in terms of v_+ .

fused ring does not exist. According to the discussion given above, NH(3) should get 600 kHz worth π electron in addition to uracil's 2311 kHz, which lead v_+ to be 2911 kHz, while v_+ of NH(1) would be substantially lower than that frequency. The v_+ frequencies for NH(7) and NH(9) are the same as those in hydroxybenzimidazole, which has the benzene instead of uracil ring. The two v_+ frequencies in 2600's would come from the 5 membered ring.

The x-ray crystallographic study shows that NH(9) involves much stronger H-bond (N—O 2.73 Å) than NH(7) (N—O 2.80 Å) [34, 35]. So one would expect that NH(9) has a higher v_0 and a rather lower v_+ .

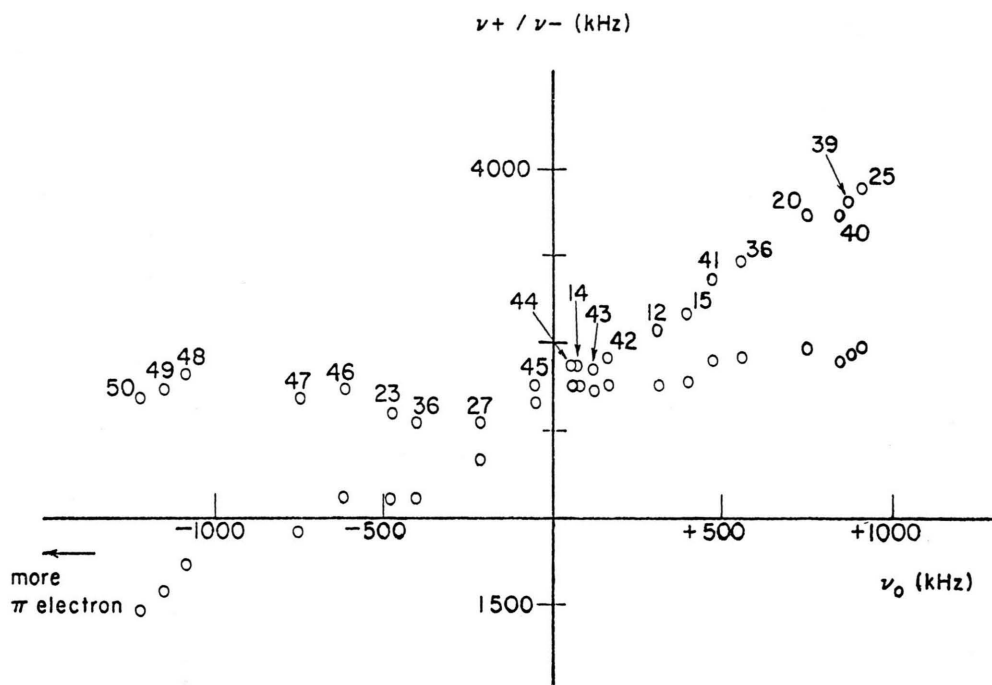


Fig. 6. Substituent effect on imino nitrogen.

frequency. The tentative spectrum assignment for uric acid is given as in Table 1.

Substituent Effect on Imino Nitrogen

As discussed in the theory section, the ν_0 transition frequency of the imino type nitrogen is proportional to the difference between the π population and the σ N–C population. Again σ N–C should be rather constant. Therefore the frequency of the imino nitrogen will be a good parameter to evaluate the π populations of the imino type nitrogens.

ν_+ and ν_- of the imino nitrogens are plotted against ν_0 in Figure 6. There is a minor axis (x, y) change caused by the sign change of the $(\sigma_{\text{NH}} - \pi)$ term in [5]. Consequently π electron rich imino nitrogens like that in cytosine (49) have a rather constant value around 2750 kHz for the ν_+ transition while π electron lacking imino nitrogens like that in pyridine (25) have the “constant” value around 2750 kHz for the ν_- transition. The constant frequencies fall in the very narrow frequency range 2550–3000 kHz. So this is very useful for spectrum assignment of a complicated ^{14}N NQR spectrum like that of 5-azacytidine (46). The ambiguous assignments of ^{14}N NQR spectra obtained by McCullen [11] turned out to be clearer thanks to the

specific frequency for the imino nitrogen. The effect of various substituents on imino nitrogen is listed in Table 10.

Fused Ring Effect

(a) α -benzene. The imino nitrogens in quinoline (20), benzothiazole (12) and benzimidazole (23) have all higher π population than pyridine (25), thiazole (41) and imidazole (27), respectively. The fused benzene ring gives substantial π electrons to the imino nitrogen in α -position. A similar π electron increase to that by fusion of imidazole and pyridine rings, respectively, is seen in azabenzimidazole (36).

(b) α -imidazole ring. The imino nitrogen of the six membered ring part in azabenzimidazole (36) has more π electron than in pyridine (25). Both of the six membered ring nitrogens in purine have also more π electron than those in pyrimidine. The π electron increase by the imidazole ring is larger than that by the fused benzene ring. This is presumably because the imidazole ring is π electron richer than the benzene ring.

(c) α -pyridine ring. The five membered imino nitrogen in azabenzimidazole (36) has substantially higher π electron density than the imino nitrogen in imid-

Table 10. Substituents Effect on Imino Nitrogens by Substances.

Substance	ph	-N=	-NH-	O 	S 	-O-	-S-	-NH ₂	others	obs. $\Delta\nu_0$	el. (10 ⁻³)
25 Pyridine ^c	-	-	-	-	-	-	-	-	-	0	0
20 Quinoline ^a	α	-	-	-	-	-	-	-	-	+151	22
43 3-Aminopyridine ^b	-	-	-	-	-	-	-	β	-	80	12
40 Pyrimidine ^b	-	β	-	-	-	-	-	-	-	136	20
36 Azabenzimidazole ^b	-	-	-	-	-	-	-	-	*	423	63
	-	-	β	-	-	-	-	-	**	1360	201
41 Thiazole ^b	-	-	-	-	-	-	β	-	-	512	76
15 α -Pyridoin ^a	-	-	-	-	-	-	-	-	***	731	108
12 Benzothiazole ^a	α	-	-	-	-	-	β	-	-	821	122
42 4-Aminopyridine ^b	-	-	-	-	-	-	-	γ	-	975	144
43 2-Aminopyrimidine ^b	-	β	-	-	-	-	-	α	-	1051	156
14 Benzoxazole ^a	α	-	-	-	-	β	-	-	-	1056	156
44 2-Aminopyridine ^b	-	-	-	-	-	-	-	α	-	1049	155
45 N-Benzylimidazole ^b	-	-	-	-	-	-	-	-	-	1162	172
	-	-	#	-	-	-	-	-	-	1111	165
27 Imidazole ^b	-	-	β	-	-	-	-	-	-	1546	229
23 Benzimidazole ^b	α	-	β	-	-	-	-	-	-	1776	263
46 5-Azacytidine ^b	-	β	# #	γ	-	-	-	α	-	1771	262
	-	β	# #	α	-	-	-	α	-	1791	265
47 5-Azauracil ^b	-	-	2 β	$\alpha + \gamma$	-	-	-	-	-	1970	292
48 N-Benzylcytosine ^b	-	-	#	α	-	-	-	α	-	2166	321
49 Cytosine ^b	-	-	β	α	-	-	-	α	-	2321	344
50 Cytidine ^b	-	-	# #	α	-	-	-	α	-	2428	360
37 Purine ^b	-	-	β	-	-	-	-	-	###	1874	278
	-	β	-	-	-	-	-	-	*	514	76
	-	β	-	-	-	-	-	-	*	484	72
18 7-Azaindole ^a	-	-	-	-	-	-	-	-	####	998	148

^a data in Table 1, ^b data in Table 4, ^c data in Table 6. * α imidazole fused. ** α pyridine fused. *** α CH(OH)-CH₂ph(OH).
 # β -NCH₂ph, ## β -Nsugar, ### α pyrimidine, #### α pyrrole fused.

azole (27). So the fused pyridine ring also acts as a π electron donor like the fused benzene or fused imidazole ring.

(d) β -fused benzene ring. The π electron density on the nitrogen in isoquinoline is substantially lower than that in pyridine. The β fused ring may act as a π electron withdrawer.

β -Imino Nitrogen: The imino nitrogens in pyrimidine (40) and 2-amino pyrimidine (43) have about the same π electron as those in pyridine (25) and 2 aminopyridine (44). On the other hand, the imino nitrogens in 5-azacytidine (46) are losing their π electrons by introducing a new imino nitrogen compared to the imino nitrogen in cytidine (50). This is presumably because the imino nitrogen in cytidine has already high π electron density.

β -Amino Nitrogen: The imino nitrogens in imidazole (27) and benzimidazole (23) have much higher π electron density than their reference compounds pyridine (25) and quinoline (20). As expected, the amino nitrogen is a good π electron donor for the imino nitrogen.

β -ring oxygen/sulfur: The nitrogen in benzoxazole (14) has more π electron density by 0.15 e than the nitrogen in quinoline (20). π electron increase is seen in benzothiazole and in thiazole (41) compared to their reference compounds quinoline (20) and pyridine (25). Both the ring oxygen and the ring sulfur are π electron donor, and the former is the more intense one.

Exocyclic amino Nitrogen: The imino nitrogens in 2-aminopyridine (44), 2-aminopyrimidine (43) and 4-aminopyridine (42) have substantially higher π electron density than those in pyridine (25), pyrimidine (40) and pyridine, respectively. On the other hand, the imino nitrogen in 3-aminopyridine (39) has about the same π electron density as that in pyridine. This shows that α - and γ -exocyclic amino groups are good π electron donors, but the β one is not. The capability of exocyclic amino groups as a π electron donors is very variable, as seen in Table 11. Substituent effects on imino nitrogen are summarized in Table 12.

The ν_+ frequencies (2900 and 3050 kHz) of the terminal amino nitrogens in allantoinic acid (6) are about

Table 11. Flexible capability of the exocyclic amino nitrogen as π electron donor.

Substance	ν_+ of ^{14}N NQR (kHz)	Change of π density (10^{-3})
Aniline	3244 ^a	Reference
Aminouracil	3282 ^b	+ 5
44 2-Aminopyridine	2970 ^c	-40
39 3-Aminopyridine	3137 ^c	-16
42 4-Aminopyridine	2967 ^c	-41
43 2-Aminopyrimidine	2784 ^c	-68
49 Cytosine	2492 ^c	-114
50 Cytidine	2476 ^c	-114
46 5-Azacytidine	2140 ^c	-164
48 N-Benzylcytosine	2280 ^c	-143
Acetamine	2105 ^d	-169
Formamide	1920 ^e	-196

^a C. T. Yim, M. A. Whitehead, and D. H. Lo, Can. J. Chem. **46**, 3595 (1968). ^b Ref. ^j in Table 4. ^c Data in Table 4. ^d D. T. Edmonds, M. J. Hunt, and A. L. Mackay, J. Magn. Reson. **9**, 66 (1973). ^e M. J. Hunt and A. L. Mackay, J. Magn. Reson. **22**, 295 (1976).

Table 12. π electron donor capabilities by substituents on cyclic imino nitrogens (in electron).



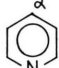
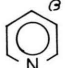
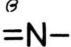

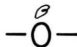
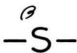
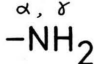
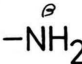
			
0.022–0.038	0.050	0.028	0
			
0	0.178	0.099	
			
0.065	0.120	0	

Table 13. Spin lattice relaxation time and averaged nuclear quadrupole coupling of solid state ^2H NMR in $\text{MgCl}_2(\text{D}_2\text{O})_6$

Temp. (K)	T_1 (s)		Correlation (time s) ^a	$e^2 Q q/h$ (kHz)	η
	38 MHz	76 MHz			
200	7×10^{-3}	1.4×10^{-2}	2.4×10^{-8}	113 (± 3)	1
170	10^{-2}	—	3.5×10^{-8}	113 (± 3)	1
100	3	—	10^{-6}	227 (± 3)	0.05 (± 0.02)

^a Correlation times were calculated based upon the T_1 equation for two site jumping (Ref. [62] and Ref. [33]).

the same as those (2970 and 2976 kHz) in 2-aminopyridine or in 4-aminopyridine. These values are substantially lower than that in aniline (3244 kHz) and are significantly higher than those in acetamide (2105 kHz) or in formamide (1920 kHz), where conjugation takes place. Therefore, there is a slight π interaction between the nitrogen and the adjacent carbon although it is not such a strong one as in acetamide or formamide.

II. Relaxation Time in the Field Cycling

^{25}Mg NQR in $\text{MgCl}_2(\text{H}_2\text{O})_6$ [9].

Although the ^1H T_1 was 600 s, which seemed long enough for the field cycling experiment, ^1H T_1 in the zero field was quite short. This resulted in a very small usable proton signal after the remagnetization. The short T_1 in the zero field may be caused by a motion of water molecules. The long ^1H T_1 at 40 MHz and the short one in the zero field suggest that the correlation time should be much longer than the reciprocal of the Larmor frequency, i.e. 10^{-6} s.

To determine whether the water molecules undergo any motion we have carried out a solid state ^2H NMR experiment on the deuterohydrate. The line-shape of the powder patterns at 170 and 200 K showed $\eta=1$, which means that the water in the hydrate undergoes the 180° flipping motion along the C2 axis rapidly. The ^2H T_1 's at 170 and 200 K were 8 and 10 ms, respectively, at 38.45 MHz. The ^2H T_1 at 76.6 MHz and 200 K was 15 ms, suggesting that the correlation time for the motion is on the slow side of the T_1 minimum. At 100 K the ^2H NMR line-shape became a pseudo static powder pattern, showing that some water molecules are nearly rigid while others are not (Figure 7). However the DQCC and η are estimated to be 227 kHz and 0.05, respectively. Using these quadrupole parameters and values for ^2H T_1 's, correlation times for the 180° flipping were calculated as listed in Table 13 [59]. It is concluded that the slow water flipping is the cause of the short T_1 in the zero field.

However, useful results were still obtained; Two clear signals were observed at 230 and 440 kHz corresponding to the transitions for ^{25}Mg . Also ^{35}Cl and ^{37}Cl quadrupole resonances were detected at 1705 and 1355 kHz, respectively. The heat capacities of ^{25}Mg , ^{35}Cl , ^{37}Cl are a very small fraction of the ^1H heat capacity and are approximately in the ratios 23:60:140. These ratios are close to the relative intensities of the NQR spectrum in Fig. 8. The existence of

180° flipping of the water molecules and the fact that multiple phase shifting of the radio frequency irradiation did not enhance the quadrupole resonance signals suggest that the signals seen for the hydrate are due to the level crossing mechanism. In this case the T_1 's of the quadrupolar nuclei are long enough to contribute to a usable ^1H magnetization.

$^{14}\text{N} \cdots ^{14}\text{N}$ Double Transitions in Parabanic Acid

Two dipolar coupled deuterons gave a six-line multiplet [59, 60] which consists of the four allowed and two forbidden transitions. In most of the deuterium NQR cases, all six lines have been observed. To date only the allowed multiplets have been reported for some dipolar coupled $^{14}\text{N} \cdots ^{14}\text{N}$ cases [62]. One of the heterocyclic compounds we studied here, parabanic acid, which has two nearly equivalent sites in the crystal, gave us an opportunity to explore the forbidden transitions. In order to search $^{14}\text{N} \cdots ^{14}\text{N}$ double transitions, a static field of 15 to 30 G was applied to wash out $^1\text{H} \cdots ^{14}\text{N}$ solid effect transitions that give a broad absorption near ^{14}N NQR. Figure 9 shows

two double transitions which correspond to

$$\nu_-(\text{site } 1) + \nu_0(\text{site } 2) \{ |XY\rangle \leftrightarrow |ZX\rangle \}$$

and

$$\nu_-(\text{site } 2) + \nu_0(\text{site } 1) \{ |YX\rangle \leftrightarrow |XZ\rangle \}$$

transitions. They are the inner doublet of the six line multiplet. To calculate the transition probability, one has to evaluate mixing coefficients which looks like

$$\langle AB | \mathcal{H}_d | BA \rangle / E, \quad (6)$$

where \mathcal{H}_d is the dipolar Hamiltonian and $E = \langle AB | H_{Q_1} + H_{Q_2} | AB \rangle - \langle BA | H_{Q_1} + H_{Q_2} | BA \rangle$. $\langle AB | \mathcal{H}_d | BA \rangle$ has non-zero elements with the dipolar B term and should be on the order of 60 Hz for the pair of ^{14}N 's in parabanic acid. Energy levels for $|YX\rangle$, $|XY\rangle$, $|YZ\rangle$, $|ZY\rangle$, $|XZ\rangle$ and $|ZX\rangle$, are -1453.1, -1463.3, 494.3, 470.0, 983.1 and 969.0 kHz, respectively. So the energy differences E , for the observed transitions are 10 and 14 kHz in parabanic acid. Therefore the probability of such transitions is at least 10^4 times smaller than the allowed transitions. ^{14}N T_1 is long enough to accumulate such transitions, resulting in a clear decrease of the ^1H magnetization even though the transition probability is small. The same kind of double transitions has been searched in cyanuric acid without success. That is presumably because E becomes 45 kHz, that is too large for detecting the transitions.

III. Motional averaging and electronic effect

Most dynamical NMR studies assume that the "static" quadrupole interaction is invariable [32, 33, 59]. However the deuterium quadrupole interaction is a function of the H-bond geometries [20–22]. Other electronic terms such as charge in the neighborhood should affect the quadrupole interaction. Therefore it is worthwhile to consider how motional averaging takes place in such cases.

The solid state ^2H NMR spectrum of the methyl group in thymine revealed an unusually high asym-

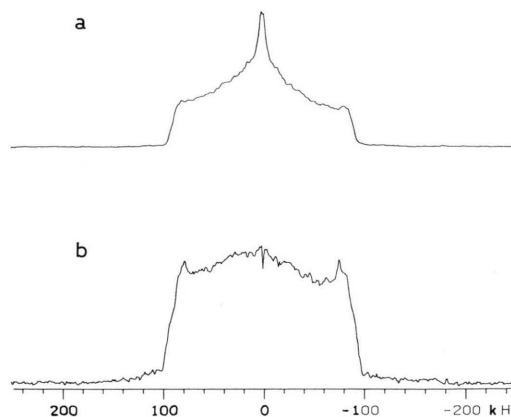


Fig. 7. Solid state deuterium spectra of $\text{MgCl}_2(\text{D}_2\text{O})_6$ at 38.4 MHz. (a) At 170 K, 160 transitions, cycle time 500 ms. (b) At 100 K, 8 transitions, cycle time 120 s [9].

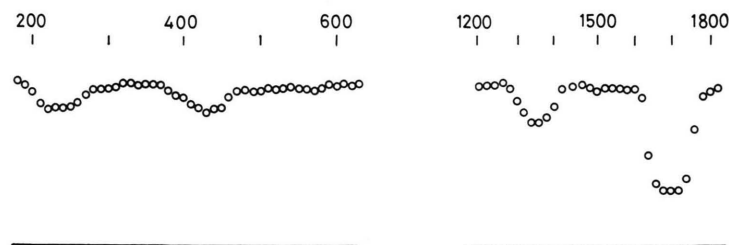


Fig. 8. ^{25}Mg , ^{35}Cl and ^{37}Cl NQR in magnesium chloride hexahydrate [9]. Transitions at 230 and 440 kHz are due to ^{25}Mg . Chlorine resonances are at 1705 and 1355 kHz.

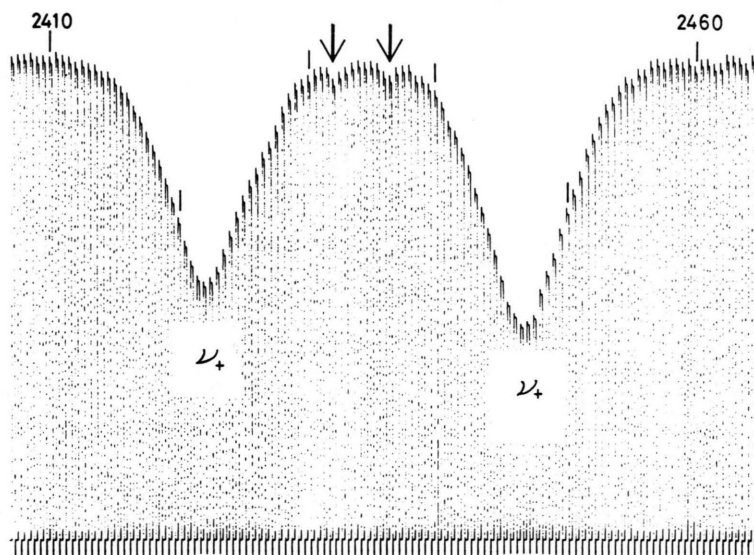


Fig. 9. ν_+ region of ^{14}N NQR spectrum of parabanic acid showing the double transitions.

Table 14. Temperature dependence of DQCC in H-bonded imidazoles. ^a Ref. [22], ^b Ref. [15].

	77 K ^a		291 K ^b	
	DQCC (kHz)	η	DQCC (kHz)	η
Imidazole				
NH	151.8	0.178	157	0.167
CH	182.8	0.088	176.9	0.068
Benzimidazole				
NH	162.7	0.144	169.7	0.139
CH	179.3	0.070	178.6	0.064

metry which has been accounted for by the negative charge on the neighboring oxygen atom [63]. Also η of the ^2H EFG tensor in perdeutero hexamethyl benzene is affected by the charge on nearest hydrogen [63]. There has been a controversy about the above two issues [64, 65]. Butler et al. predicted that the ^2H EFG tensor is a good indicator of the charge densities of neighboring atom [66].

Let us consider motional averaging of deuterium cases in H-bonded systems.

Small Amplitude Motion in Imidazoles

Table 14 lists published ^2H quadrupole parameters of the crystalline imidazoles, where strong $\text{NH} \cdots \text{N}$ H-bonds occur.

The DQCC's of the CH sites in the imidazoles at 291 K are smaller than at 77 K by a fraction suggesting that the aromatic rings undergo a small amplitude motion. On the other hand the DQCC's of the H-bonded NH sites at 291 K are significantly larger than those at 77 K. This phenomenon may be accounted for by breakdown of the hydrogen bond by the motion, since the DQCC becomes larger when no H-bond exists.

We have employed a model of equally populated two site jumps with full angle of θ (Figure 10). It is also assumed that the second DQCC becomes larger at a constant rate up to 50% of the original DQCC. Space averaged DQCC's have been obtained by diagonalizing the averaged EFG:

$$\text{Averaged EFG} = 0.5 \cdot (\text{EFG 1}) + 0.5 \cdot R^{-1}(\text{EFG 2}) R. \quad (7)$$

Figure 11 illustrates the assumed EFG 2 simulating the breakdown of H-bonds. The numerical calculation indicated that the averaged DQCC will go up and show a maximum at $\theta = 20^\circ$ to 30° as shown in Figure 12.

— ND_3 Motion in p-Fluoro-DL-phenylalanine (PFF) [33]

The ^2H powder spectrum of D_3PFF at 22°C is shown in Figure 13. A good computer simulation was obtained by summing three powder patterns. The re-

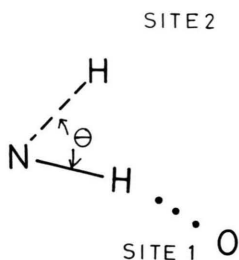


Fig. 10. Two site jumps model. Site 2 has larger DQCC compared to site 1 depending on the angle θ .

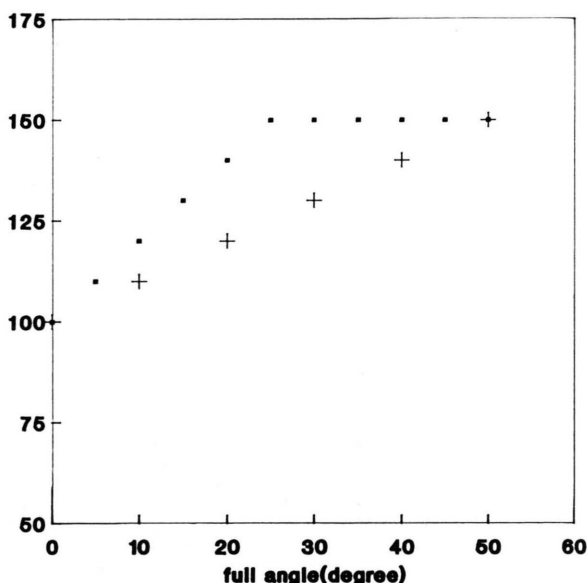


Fig. 11. DQCC for the second site to simulate breakdown of H-bond. ■ represents 20% increase per 10 deg. in θ . + represents 10% increase per 10 deg. in θ .

spective coupling constants (and asymmetry parameters) were 167 kHz (0.02), 167 kHz (0.02) and 129 kHz (0.05). These DQCC's are consistent with the H-bonded $N \cdots O$ distances given in the X-ray study [33]. The powder spectrum at 150°C (Fig. 13) has been considered a single powder pattern having DQCC = 48 kHz, $\eta = 0.37$. This ^2H EFG tensor can be obtained by three-site jumps (rather than diffusional motion) of an NH_3 group having the static EFG parameters which were obtained at 22°C.

Thymidine ND Spectrum [67]

It has been reported that the base position of thymidine is essentially static while the deoxyribose ring undergoes large amplitude motion (Figure 14).

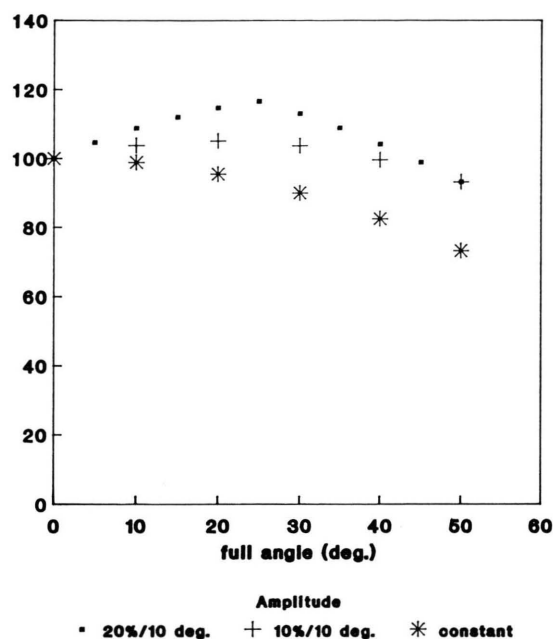


Fig. 12. Averaged DQCC based upon the two site jumps with the second DQCC larger than the first DQCC.

This gave us a unique situation, that is the NH bond vector sits still while the H-bond breaks down. This corresponds to the model shown in Fig. 10 with $\theta = 0^\circ$.

The powder ^2H NMR spectrum of (d_3 -3,3'(OD), 5'(OD)) thymidine at 22°C is a superposition of three powder patterns (Figure 15). A room temperature X-ray structure showed that H-bond lengths, $\text{YH} \cdots \text{Y}$, are 2.74, 2.79, and 2.85 Å for the 3', 5', and 3 positions respectively [68]. Based upon the empirical relationship between $\text{XD} \cdots \text{Y}$ lengths and DQCC [21, 22], the position 3 (ND \cdots O) was clearly distinguished from the others in terms of singularity positions (marked in Fig. 15) in the superimposed powder spectrum.

The ^2H NMR spectrum of (d_3 -3,3'(OD), 5'(OD)) thymidine at 75°C (Fig. 15) differs from the spectrum at 22°C; in two respects: (1) the intensity decreased by a factor of 2.5 upon going from 22 to 75°C and (2) the overall breadth of the powder spectrum increased by 20 kHz from 22 to 75°C. The base being rigid, the total loss of signal can be attributed to short T_2 at the 3' and 5' positions caused by a large amplitude slow motion. Whether or not this motion is the one that was observed at the C2' position is not determined because there are other possible rotations such as either along the C3'-O3' axis or the C4'-C5' axis. At 22°C, the 3 position ($\text{N}-^2\text{H}$) makes a H-bond to the

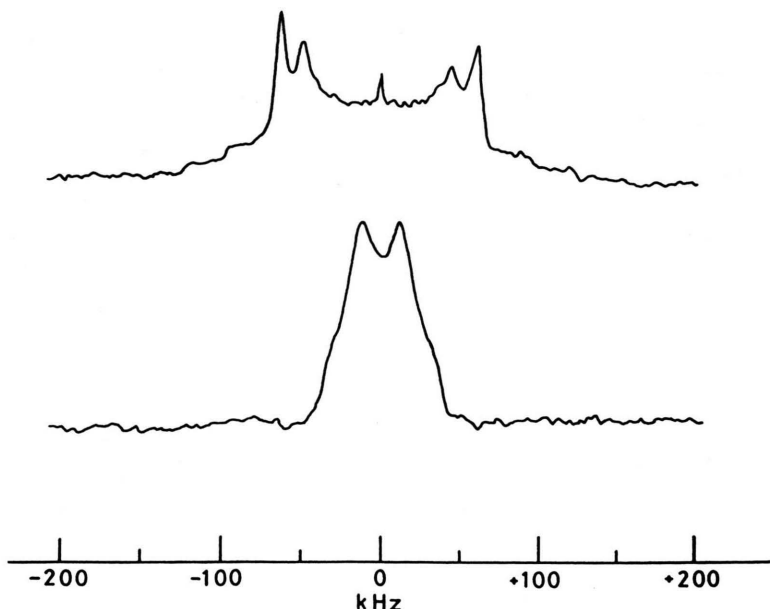


Fig. 13. Solid state ^2H NMR spectrum of $\text{d}_3(\text{ND}_3)$ p-fluoro-D,L-phenylalanine. (a) at 22°C , (b) at 150°C .

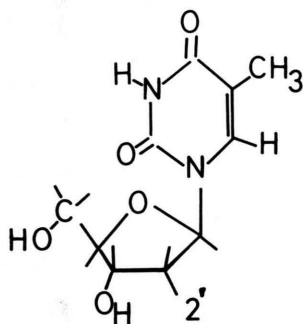


Fig. 14. Molecular structure of thymidine. The deoxyribose ring was found to undergo large amplitude slow motion while the base position is essentially static. (refs. [63] and [65])

$3'$ oxygen of a neighboring molecule in the crystal [68]. However at the high temperature, the $3'$ oxygen may not be available for H-bond formation because of the large amplitude motion of the deoxyribose ring. ^2H 's with no H-bonded $\text{N}-^2\text{H}$ have a larger DQCC (over 200 kHz) than the H-bonded ones [21, 22]. Therefore the absence of H-bonding at high temperature presumably causes the larger breadth of the powder spectrum observed at 75°C as compared with that at 22°C .

Acknowledgements

The author would like to thank Professors Eiji Niki, Theodore L. Brown and Drs. Dennis A. Torchia

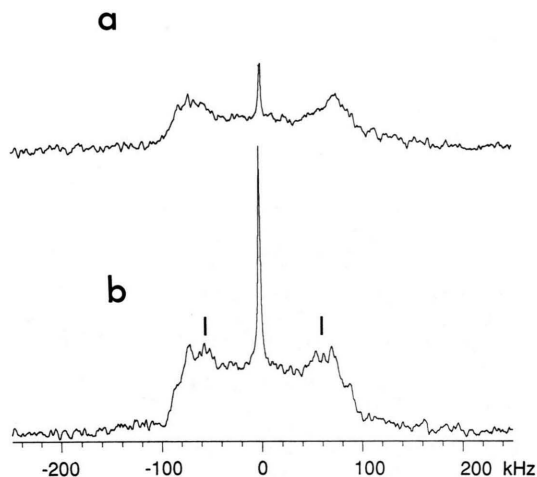


Fig. 15. Solid state ^2H NMR spectrum of $(\text{d}_3\text{-}3(\text{ND}), 3'(\text{OD}), 5'(\text{OD}))$ thymidine at (a) 75°C and (b) 22°C . The marked singularities are due to the ND site.

and Akio Sonoda for encouragement and helpful discussions.

The work presented has been supported by Grants from the Ministry of Education (Japan), by Grant GM 23395 from the National Institutes of Health (USA) and by the intramural research program of the National Institute of Dental Research. Computational time of VAX 8350 at Upjohn Tsukuba Laboratories is also acknowledged.

- [1] E. A. C. Lucken, *Nuclear Quadrupole Coupling Constants*, Academic Press, London 1968.
- [2] R. E. Slusher and E. L. Hahn, *Phys. Rev.* **166**, 332 (1968).
- [3] D. T. Edmonds, *Phys. Reports* **290**, 234 (1977).
- [4] T. L. Brown, L. G. Butler, D. Y. Curtin, Y. Hiyama, I. C. Paul, and R. B. Wilson, *J. Amer. Chem. Soc.* **104**, 1172 (1982).
- [5] L. G. Butler and T. L. Bown, *J. Magn. Reson.* **42**, 120 (1981).
- [6] T. L. Brown, *J. Mol. Struct.* **58**, 293 (1980).
- [7] L. G. Butler, C. P. Cheng, and T. L. Brown, *J. Phys. Chem.* **85**, 2738 (1981).
- [8] D. T. Edmonds and J. P. G. Mailer, *J. Magn. Reson.* **36**, 411 (1979).
- [9] Y. Hiyama, P. M. Woyciesjes, T. L. Brown, and D. A. Torchia, *J. Magn. Reson.* **72**, 1 (1987).
- [10] D. T. Edmonds and P. A. Speight, *Phys. Lett.* **34A**, 325 (1971).
- [11] W. L. McCullen, Ph.D. Thesis, University of Illinois, 1981.
- [12] Y. Hiyama, L. G. Butler, W. A. Olsen, and T. L. Brown, *J. Magn. Reson.* **44**, 483 (1981).
- [13] E. A. Keiter, Y. Hiyama, and T. L. Brown, *J. Mol. Struct.* **111**, 1 (1983).
- [14] M. Redshaw, M. H. Palmer, and R. H. Findlay, *Z. Naturforsch.* **34A**, 220 (1979).
- [15] M. L. Garcia, J. A. S. Smith, P. M. G. Bavin, and C. R. Ganellin, *J. Chem. Soc. Perkin II*, 1391 (1983).
- [16] M. L. Garcia and J. A. S. Smith, *J. Chem. Soc. Perkin II*, 1401 (1983).
- [17a] E. Schempp and P. J. Bray, *Phys. Lett.* **25A**, 414 (1967).
- [17b] C. Tarimci and E. Schempp, *Acta Cryst.* **B33**, 240 (1977).
- [18] L. Guibe and E. A. C. Lucken, *Mol. Phys.* **14**, 73 (1968).
- [19] T. Maruizumi, Y. Hiyama, N. Watanabe, and E. Niki, *Bull. Chem. Soc. Jpn.* **51**, 978 (1978).
- [20] G. Soda and T. Chiba, *J. Chem. Phys.* **50**, 439 (1969).
- [21] M. J. Hunt and A. L. Mackay, *J. Magn. Reson.* **15**, 402 (1974).
- [22] Y. Hiyama, E. A. Keiter, and T. L. Brown, *J. Magn. Reson.* **67**, 202 (1986).
- [23] C. H. Townes and B. P. Dailey, *J. Chem. Phys.* **17**, 782 (1949).
- [24] S. Onda, H. Harada, D. Nakamura, and M. Kubo, *J. Magn. Reson.* **8**, 238 (1972).
- [25] S. R. Rabbani, D. T. Edmonds, and P. Gosling, *J. Magn. Reson.* **72**, 422 (1987).
- [26] R. E. Stark, R. A. Haberkorn, and R. G. Griffin, *J. Chem. Phys.* **68**, 1996 (1978).
- [27] J. G. Hexem, M. H. Frey, and S. J. Opella, *J. Chem. Phys.* **77**, 3847 (1982).
- [28] A. Naito, S. Ganapathy, and C. A. McDowell, *J. Magn. Reson.* **48**, 367 (1982).
- [29] C. P. Cheng and T. L. Brown, *J. Am. Chem. Soc.* **101**, 2327 (1979).
- [30] L. G. Butler, Ph.D. Thesis, University of Illinois, 1981.
- [31] D. A. D'Avingnon, Ph.D. Thesis, University of Illinois, 1980.
- [32] S. K. Sarkar, C. E. Sullivan, and D. A. Torchia, *J. Biol. Chem.* **258**, 9762 (1983).
- [33] Y. Hiyama, J. V. Silverton, D. A. Torchia, J. T. Gerig, and S. J. Hammond, *J. Amer. Chem. Soc.* **108**, 2715 (1986).
- [34] D. R. Davies and J. J. Blum, *Acta Cryst.* **8**, 129 (1955).
- [35] B. M. Craven and R. K. McMullan, *Acta Cryst.* **B35**, 934 (1979).
- [36] H. Ringertz, *Acta Cryst.* **20**, 397 (1966).
- [37] A. Escande, J. L. Galigne, and J. Lapasset, *Acta Cryst.* **B30**, 1490 (1974).
- [38] G. R. Form, E. S. Raper, and T. C. Downie, *Acta Cryst.* **B32**, 345 (1976).
- [39] P. Groth, *Acta Chem. Scand.* **27**, 945 (1973).
- [40] T. Ashida, S. Hirokawa, and Y. Okaya, *Acta Cryst.* **18**, 122 (1965).
- [41] H. W. Ehrlich, *Acta Cryst.* **18**, 122 (1965).
- [42] T. LaCour and S. E. Rasmussen, *Acta Chem. Scand.* **27**, 1845 (1973).
- [43] T. L. Brown and C. P. Cheng, *Faraday Symposia of the Chemical Society* **13**, 75 (1978).
- [44] a) G. C. Verschoor, *Nature London* **202**, 1206 (1964).
b) P. Coppens and A. Vos, *Acta Cryst.* **B27**, 146 (1971).
c) P. Verschoor and E. Keulen, *Acta Cryst.* **B27**, 134 (1971).
d) A. Kutoglu and E. Hellner, *Acta Cryst.* **B34**, 1617 (1978).
- [45] T. P. Das and E. L. Hahn, *Nuclear Quadrupole Resonance Spectroscopy*, Solid State Phys. Suppl. 1, Seitz and Turnbull, eds. Academic, New York 1958, Chapter 3.
- [46] J. Koo and Y. N. Hsieh, *Chem. Phys. Lett.* **9**, 238 (1971).
- [47] D. T. Edmonds and P. A. Speight, *J. Magn. Reson.* **12**, 134 (1973).
- [48] G. L. Blackmann, R. D. Brown, F. R. Burden, and I. R. Elsum, *J. Mol. Spectros.* **60**, 63 (1976).
- [49] S. Martinez-Carrera, *Acta Cryst.* **20**, 783 (1966).
- [50] R. K. McMullan, J. Epstein, J. R. Ruble, and B. M. Craven, *Acta Cryst.* **B35**, 688 (1979).
- [51] L. G. Butler and T. L. Brown, *J. Amer. Chem. Soc.* **103**, 6541 (1981).
- [52] S. Ikuta, S. Hashimoto, and M. Imamura, *Int. J. Quant. Chem.* **18**, 515 (1980).
- [53] M. J. S. Dewar, A. J. Harget, N. Trinajstic, and S. D. Worley, *Tetrahedron* **26**, 4505 (1970).
- [54] L. Klasinc, E. Pop, N. Trinajstic, and J. V. Knop, *Tetrahedron* **28**, 3465 (1972).
- [55] J. Koller, A. Azman, and N. Trinajstic, *Z. Naturforsch.* **29A**, 624 (1974).
- [56] Y.-N. Hsieh, G. V. Rubenacker, C. P. Cheng, and T. L. Brown, *J. Amer. Chem. Soc.* **99**, 1384 (1977).
- [57] G. V. Rubenacker and T. L. Brown, *Inorg. Chem.* **19**, 392 (1980).
- [58] D. T. Edmonds and A. A. L. White, *J. Magn. Reson.* **31**, 149 (1978).
- [59] D. A. Torchia and A. Szabo, *J. Magn. Reson.* **49**, 107 (1982).
- [60] I. J. F. Pople, *Adv. Nucl. Quadr. Reson.* **4**, 115 (1980).
- [61] N. Hadipour and J. L. Ragle, *Z. Naturforsch.* **40a**, 335 (1985).
- [62] S. Kurita and Y. Abe, *J. Mol. Struct.* **58**, 535 (1980).
- [63] Y. Hiyama, S. Roy, K. Guo, L. G. Butler, and D. A. Torchia, *J. Amer. Chem. Soc.* **109**, 2525 (1987).
- [64] C. Schmidt, B. Blümich, and H. W. Spiess, *J. Magn. Reson.* **79**, 269 (1988).
- [65] A. Kintanar, T. M. Alam, W.-C. Huang, D. C. Shindele, D. E. Wemmer, and G. Drobny, *J. Amer. Chem. Soc.* **110**, 6367 (1988).
- [66] M. A. Jackisch, W. L. Jarrett, K. Guo, F. R. Fronczek, and L. G. Butler, *J. Amer. Chem. Soc.* **110**, 343 (1988).
- [67] Y. Hiyama, S. Roy, J. S. Cohen, and D. A. Torchia, *J. Amer. Chem. Soc.* **111**, 8609 (1989).
- [68] D. W. Young, P. Tollin, and H. R. Wilson, *Acta Cryst.* **B25**, 1423 (1969).